Progress In Electromagnetics Research, Vol. 124, 71–83, 2012

DESIGN ANALYSIS OF A BEAM SPLITTER BASED ON THE FRUSTRATED TOTAL INTERNAL REFLECTION

J.-R. Chang Chien[1], C.-C. Liu[2], C.-J. Wu[3,*], P.-Y. Wu[3], and C.-C. Li[3]

[1]Department of Electronic Engineering, National Kaohsiung First University of Science and Technology, Kaohsiung 811, Taiwan, R.O.C.

[2]Department of Electro-Optical Engineering, National Formosa University, Yunlin 632, Taiwan, R.O.C.

[3]Institute of Electro-Optical Science and Technology, National Taiwan Normal University, Taipei 116, Taiwan, R.O.C.

Abstract—In this work, a theoretical analysis on the design of the beam splitter (BS) based on the frustrated total internal reflection (FTIR) is made. We consider a model structure made of a low-index gap layer bounded by two high-index layers. In the design of a 50/50 BS, we find that there exists a critical gap thickness which is a decreasing function of the angle of incidence for both TE and TM waves. There also exists a critical wavelength for the incident wave, and it increases with increasing angle of incidence. Finally, at a fixed gap thickness and wavelength of incident wave, the critical angle in TE wave is slightly larger than that of TM wave. The analysis provides some fundamental information that is of particular use to the design of a BS within the framework of FTIR.

1. INTRODUCTION

Total internal reflection (TIR) is an optical phenomenon which occurs when a wave is incident at an angle greater than the critical angle from denser medium n_1 onto a rarer medium n_2, with $n_1 > n_2$. Under TIR, the incident wave is completely reflected because the transmitted wave is evanescent and no power transmitted into medium 2. An important and fundamental property of the reflected wave is the occurrence of

Received 9 November 2011, Accepted 1 January 2012, Scheduled 12 January 2012

* Corresponding author: Chien-Jang Wu (jasperwu@ntnu.edu.tw).

the Goos-Hanchen shift [1]. TIR is known as the main mechanism for the wave transmission in the optical fiber. In practical application, an additional medium 3 of refractive index $n_3 > n_2$ is introduced to limit region 2 in space $0 < x < d_2$, as illustrated in the lower panel of Figure 1. If the thickness of medium 2 is small enough, then it is possible to have a transmitted wave in medium 3, leading to the so-called optical tunneling. In this case, total internal reflection does not hold again, and reflectance is forced to be less than unity. As a result, we have the so-called frustrated total internal reflection (FTIR) [2]. Experimental verification of FTIR is available [3]. A novel reflective image display based on the use of FTIR is available [4].

Based on the use of FTIR, in this work, we shall develop the theory of beam splitter (BS). Beam splitters (BSs), for which both the transmitted and reflected beams are equally important to be utilized, are essential optical components which are widely used in optical instruments, lasers, electro-optic displays, optical recording, etc. [5]. They can also be used in polarization-based optical systems such as the ellipsometers, magneto-optic data storage devices, and free-space optical switching networks [6–9]. A block diagram of BS is sketched in the upper panel of Figure 1, where it has an input and two outputs. The input optical beam has a intensity of I_i, and the two outputs have the intensities $I_{o,1}$ and $I_{o,2}$, respectively. Our goal is to design a 50/50 BS, i.e., $I_{o,1} = I_{o,2} = 0.5I_i$. The one-input and two-output

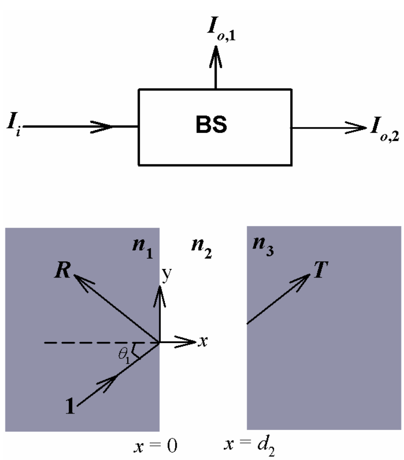

Figure 1. The block diagram of a BS (upper panel) and its model structure based on the FTIR (lower panel). Here, $n_1 > n_2$, $n_3 > n_2$, and the thickness of low-index layer is d_2.

system is modeled as a FTIR structure in the lower panel of Figure 1, where the input beam has a unit power, and the two outputs of BS are represented by reflectance R and transmittance T, respectively. In fact, the relationships between R, T and I_i, $I_{o,1}$, $I_{o,2}$ are defined as $R = I_{o,1}/I_i$, and $T = I_{o,2}/I_i$. A 50/50 BS means $R = T = 0.5$, which is possible to be achieved by making use of the mechanism of FTIR.

In what follows, we first present a general theoretical description on the calculation of response functions R and T, including TE and TM waves as well. Next, we limit to the practical case where the angle of incidence is taken at 45° together with $n_1 = n_3$. Explicitly analytical expressions, which are of use to determine the gap width and/or wavelength of the incident wave, are derived for both TE and TM waves in a 50/50 BS. Then, we give analytical results on the response functions R and T as functions of gap width, wavelength of the incident wave, and the angle of incidence. The results demonstrate how a 50/50 BS can be achieved by suitably selecting the parameters, such as the gap width, the wavelength of the incident wave, and the angle of incidence.

2. BASIC EQUATIONS

Let us consider the model structure in the lower panel of Figure 1, in which the low-index layer n_2 is bounded by two high-index layers of n_1 and n_3, i.e., $n_1 > n_2$ and $n_3 > n_2$. It is worth mentioning that, in order to achieve FTIR, the thickness of low-index layer 2 (also called the gap layer) d_2 must be much less than the wavelength of the incident wave. The incident wave, the input signal, is launched in medium 1 at an angle of incidence θ_1 which has to be greater than the critical angle $\theta_c = \sin^{-1}(n_2/n_1)$. The two output signals are taken to the reflected and transmitted waves which have the response functions represented by reflectance R and transmittance T, respectively. The system can work as a 50/50 BS only when the condition, $R = T = 0.5$, occurs. With a half power in each splitting beam, the 50/50 BS is also referred to as a 3-dB BS.

To determine the response functions of R and T, we shall use the transfer matrix method (TMM) [2]. The TMM has been known as an elegant method and widely employed to the study of layered structures, including metamaterials [10–19]. In describing the TMM formulae, the temporal part is assumed to be $\exp(j\omega t)$ for all fields. For a three-medium system in Figure 1, the total system matrix is expressed as

$$\mathbf{M} = \begin{pmatrix} M_{11} & M_{12} \\ M_{21} & M_{22} \end{pmatrix} = D_1^{-1} D_2 P_2 D_2^{-1} D_3, \tag{1}$$

where the dynamical matrix D_i ($i = 1, 2, 3$), is written as

$$D_i = \begin{pmatrix} 1 & 1 \\ n_i \cos\theta_i & -n_i \cos\theta_i \end{pmatrix}, \tag{2}$$

for TE wave, and

$$D_i = \begin{pmatrix} \cos\theta_i & \cos\theta_i \\ n_i & -n_i \end{pmatrix}, \tag{3}$$

for TM wave, respectively. The propagation matrix P_2 in Equation (1) for the gap layer 2 takes the form

$$P_2 = \begin{pmatrix} \exp(jk_2 d_2) & 0 \\ 0 & \exp(-jk_2 d_2) \end{pmatrix}, \tag{4}$$

where d_2 is the thickness of layer 2 and the wave number $k_2 = n_2\omega \cos\theta_2/c$. The ray angles θ_2 and θ_3 are related to the incident angle θ_1 by the Snell's law of refraction, i.e.,

$$n_1 \sin\theta_1 = n_2 \sin\theta_2 = n_3 \sin\theta_3. \tag{5}$$

Having obtained the matrix elements in Equation (1), the reflection and transmission coefficients can be calculated by the following equations, namely

$$r = \frac{M_{21}}{M_{11}}, \quad t = \frac{1}{M_{11}}. \tag{6}$$

The corresponding reflectance R and transmittance T are thus given by

$$R = |r|^2 = \left|\frac{M_{21}}{M_{11}}\right|^2, \tag{7}$$

$$T = \frac{n_3 \cos\theta_3}{n_1 \cos\theta_1}|t|^2 = \frac{n_3 \cos\theta_3}{n_1 \cos\theta_1}\left|\frac{1}{M_{11}}\right|^2. \tag{8}$$

By direct manipulation in Equation (1), expressions for the matrix elements M_{11} and M_{12} can be obtained, with the results,

$$M_{11} = \frac{1}{2}\left(1 + \frac{n_3 \cos\theta_3}{n_1 \cos\theta_1}\right)\cos\phi_2 + j\frac{1}{2}\sin\phi_2\left(\frac{n_3 \cos\theta_3}{n_2 \cos\theta_2} + \frac{n_2 \cos\theta_2}{n_1 \cos\theta_1}\right), \tag{9}$$

$$M_{21} = \frac{1}{2}\left(1 - \frac{n_3 \cos\theta_3}{n_1 \cos\theta_1}\right)\cos\phi_2 - j\frac{1}{2}\sin\phi_2\left(\frac{n_2 \cos\theta_2}{n_1 \cos\theta_1} - \frac{n_3 \cos\theta_3}{n_1 \cos\theta_1}\right), \tag{10}$$

for TE wave, and

$$M_{11} = \frac{1}{2}\left(\frac{\cos\theta_3}{\cos\theta_1} + \frac{n_3}{n_1}\right)\cos\phi_2 + j\frac{1}{2}\sin\phi_2\left(\frac{n_2 \cos\theta_3}{n_1 \cos\theta_2} + \frac{n_3 \cos\theta_2}{n_2 \cos\theta_1}\right), \tag{11}$$

$$M_{21} = \frac{1}{2}\left(\frac{\cos\theta_3}{\cos\theta_1} - \frac{n_3}{n_1}\right)\cos\phi_2 - j\frac{1}{2}\sin\phi_2\left(\frac{n_2 \cos\theta_3}{n_1 \cos\theta_2} - \frac{n_3 \cos\theta_2}{n_2 \cos\theta_1}\right), \tag{12}$$

for TM wave, respectively.

Before presenting the analytical results for the design of a 50/50 BS, let us consider a practical case, i.e., $\theta_1 = 45°$, and $n_1 = n_3$. With $\theta_1 > \theta_c$, $\sin\theta_2 > 1$, $\cos\theta_2$ is thus complex-valued and takes the form,

$$n_2 \cos\theta_2 = -j\sqrt{\frac{n_1^2}{2} - n_2^2}. \tag{13}$$

In this case, explicitly analytical expressions for reflectance and transmittance can be obtained, namely

$$R_{TE} = \frac{\left(1-\alpha^2\right)^2 \sinh^2(\beta d_2) + 4\alpha^2 \sinh^2(\beta d_2)}{(1-\alpha^2)^2 \sinh^2(\beta d_2) + 4\alpha^2 \cosh^2(\beta d_2)}, \tag{14}$$

$$T_{TE} = \frac{4\alpha^2}{(1-\alpha^2)^2 \sinh^2(\beta d_2) + 4\alpha^2 \cosh^2(\beta d_2)}, \tag{15}$$

for TE wave, and

$$R_{TM} = \frac{\left(\frac{n_1^2}{n_2^2} - \frac{n_2^2}{n_1^2}\alpha^2\right)^2 \sinh^2(\beta d_2) + 4\alpha^2 \sinh^2(\beta d_2)}{\left(\frac{n_1^2}{n_2^2} - \frac{n_2^2}{n_1^2}\alpha^2\right)^2 \sinh^2(\beta d_2) + 4\alpha^2 \cosh^2(\beta d_2)}, \tag{16}$$

$$T_{TM} = \frac{4\alpha^2}{\left(\frac{n_1^2}{n_2^2} - \frac{n_2^2}{n_1^2}\alpha^2\right)^2 \sinh^2(\beta d_2) + 4\alpha^2 \cosh^2(\beta d_2)}, \tag{17}$$

for TM wave, where

$$\alpha = \frac{n_1}{\sqrt{n_1^2 - 2n_2^2}}, \quad \beta = k_0\sqrt{\frac{n_1^2}{2} - n_2^2}, \tag{18}$$

where $k_0 = \omega/c$ with c being the speed of light in vacuum. For obtaining 50/50 beam splitting, it is required to have $T_{TE,TM} = 0.5$, which in turn leads to

$$\sinh(\beta d_2) = \frac{2\alpha}{1+\alpha^2} \ (TE \text{ wave}), \tag{19}$$

and

$$\sinh(\beta d_2) = \frac{2\alpha}{\sqrt{\left(\frac{n_1^2}{n_2^2} - \frac{n_2^2}{n_1^2}\alpha^2\right)^2 + 4\alpha^2}} \ (TM \text{ wave}), \tag{20}$$

according to Equations (15) and (17), respectively. Equation (19) agrees with the recent report by Drevko and Zyuryukin [20]. Equations (19) and (20) are simple and of particular use in determining the gap width d_2 of the low-index layer 2 and/or the wavelength of incidence wave when the angle of incidence is fixed at 45°.

3. NUMERICAL RESULTS AND DISCUSSION

3.1. Determination of Gap Thickness for 50/50 BS

Let us now present the analytical results for the design of a 50/50 BS. We take $n_1 = n_3 = 1.5$ (glass) and $n_2 = 1$. The critical angle is thus calculated to be $\theta_c = \sin^{-1}(1/1.5) = 42°$. We first fix the wavelength of the incident wave at $\lambda = 500\,\text{nm}$. We explore the critical thickness of the gap layer 2 under different angles of incidence. In Figure 2, we plot the reflectance and transmittance as a function of gap thickness d_2 for both the TE wave (a) and TM wave (b), respectively, at $\theta_1 = 45°$, $60°$, and $75°$. It can be seen that both transmittance and reflectance curves intersect at a critical thickness $d_2 = d_c$ (marked by the vertical arrow) at which $R = T = 0.5$, a required condition of 50/50 BS. For thickness smaller than d_c, transmittance is greater than reflectance, whereas transmittance will be less than reflectance for thickness larger than d_c. The values of d_c are: $d_c/\lambda = 0.26$ (45°), 0.17 (60°), 0.09 (75°)

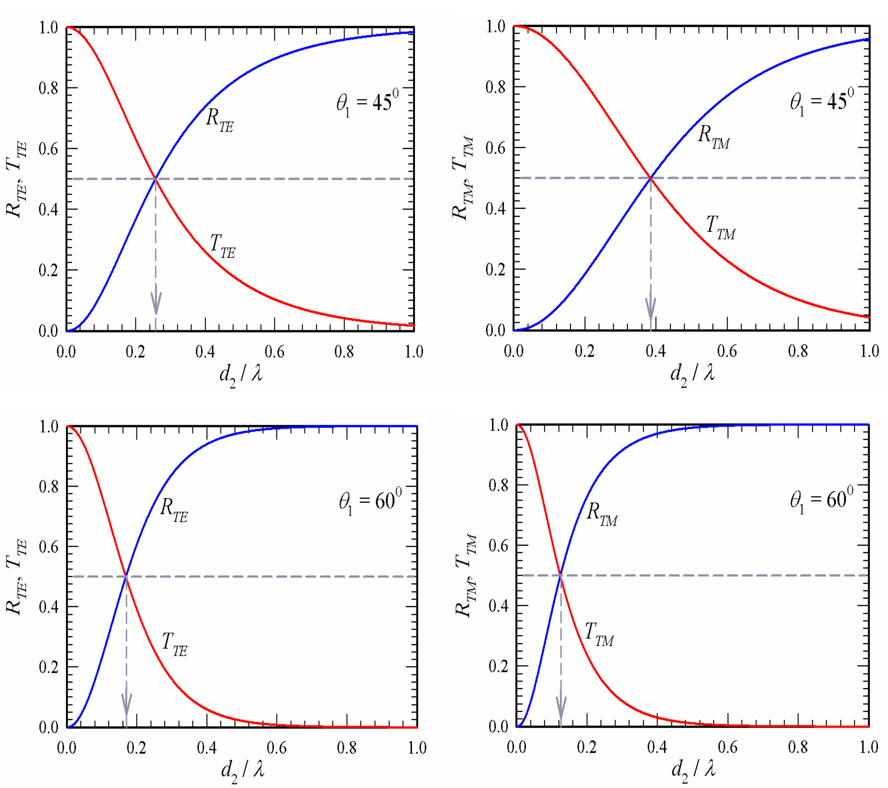

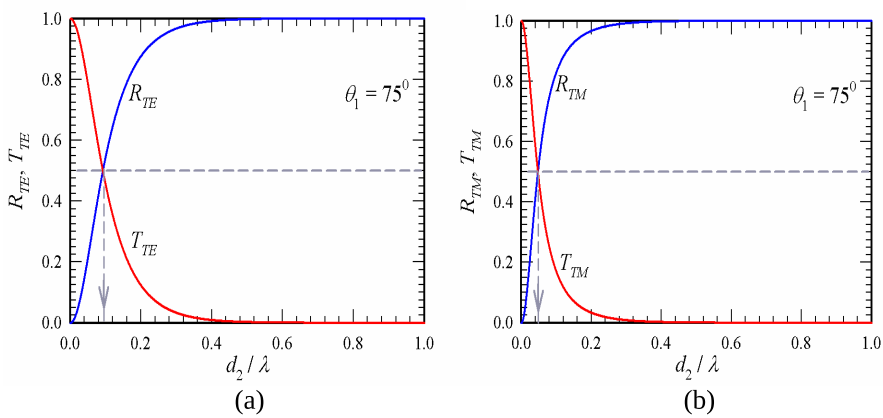

Figure 2. The calculated reflectance and transmittance as a function of gap thickness d_2 at $\lambda = 500\,\mathrm{nm}$. Here, (a) is for the TE wave and (b) is for the TM wave, respectively.

Table 1. The calculated critical thickness of gap layer at some selected angles of incidence for both the TE and TM waves.

		43°	45°	50°	55°	60°	65°	70°	75°	80°	85°
d_c/λ	TE	0.28	0.26	0.22	0.19	0.17	0.14	0.12	0.09	0.07	0.03
	TM	0.51	0.38	0.24	0.17	0.12	0.09	0.07	0.05	0.03	0.015

for TE wave and 0.38 (45°), 0.12 (60°), 0.05 (75°) for TM wave, as can also be seen in Table 1. The critical thickness decreases with the increase in the angle of incidence for both TE and TM waves. In fact, the critical thickness $d_c/\lambda = 0.26$ at 45° in TE wave can be easily found by Equation (19). Similarly, $d_c/\lambda = 0.38$ for TM wave agrees with Equation (20).

Table 1 gives some values of critical thickness at some selected angles of incidence for both TE and TM waves. These values are summarized in Figure 3. Some features are of note. First, at angle near the critical angle (42°), the critical thickness for obtaining BS in TM wave is greater than that in TE wave. Second, it is of interest to see that both have a crossover at $\theta_1 = 52.6°$, and $d_c/\lambda = 0.21$ (indicated by two gray arrows). At this crossing point, both TE and TM waves of incidence can equally make the system work as a 50/50 BS. This special point enables us to obtain two circularly polarized splitting beams by launching an incident wave of circular polarization. Third, at an angle larger than 52.6°, the critical thickness for TE wave is larger than that in TM wave.

3.2. Determination of Wavelength for 50/50 BS

We next fix the gap thickness at $0.2\lambda_0$ ($\lambda_0 = 500\,\text{nm}$). We plot the R and T in the wavelength domain (from 100–1200 nm) from which a 50/50 BS can be obtained at a critical wavelength λ_c which is indicated by the vertical arrow. The results are shown in Figure 4. It can be seen from the figure that λ_c increases fast with increasing angle of incidence for both TE and TM waves. In addition, based on the curve of transmittance, the system can be regarded as a low-pass filter since it transmits long wavelength only. Moreover, it should be mentioned that, in TM wave, we show the results of R and T at 65° rather than at 75° because the crossover point is far more than 1200 nm at 75°, out

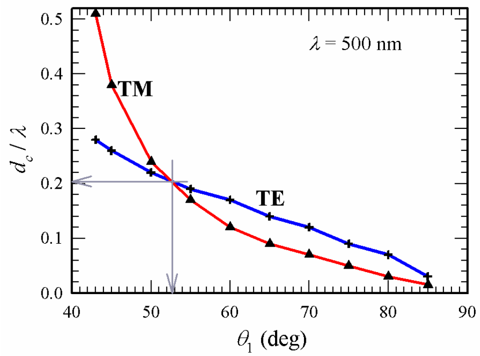

Figure 3. The calculated critical thickness as a function of the angle of incidence for the 50/50 beam splitting. Both TE and TM curves have an intersection at $\theta_1 = 52.6°$, and $d_c/\lambda = 0.21$.

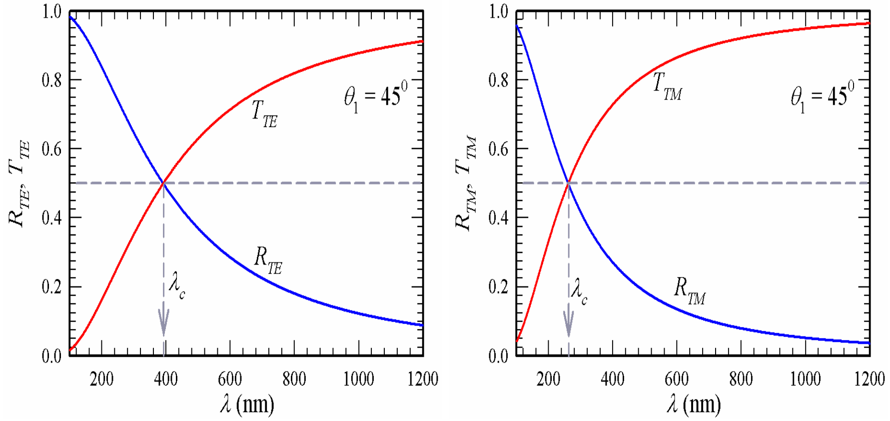

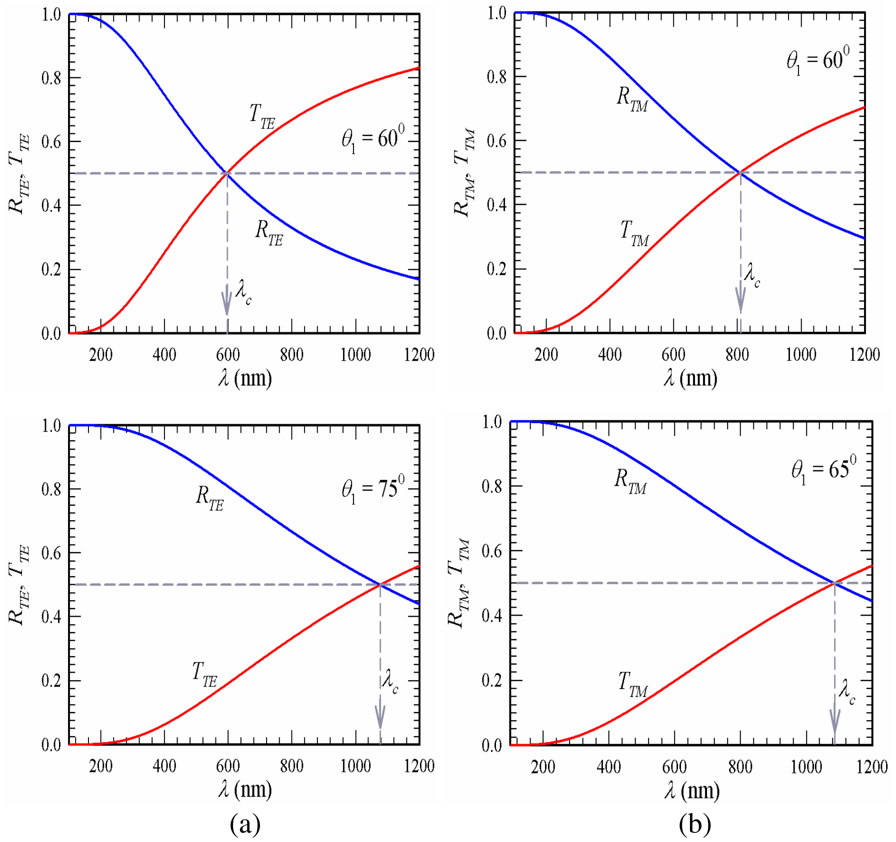

Figure 4. The calculated wavelength-dependent reflectance and transmittance for the TE wave ((a) at 45°, 60°, and 75°) and the TM wave ((b) at 45°, 60°, 65°).

of the range of Figure 4. Some values of λ_c are given in Table 2, and its increasing trend with the angle of incidence is shown in Figure 5. We see that both treads in TE and TM waves have a crossover at $\theta_1 = 51.8°$ at which $\lambda_c = 478\,\text{nm}$. This crossover point can be applied to preserve the polarization state for the two splitting beams when the incident wave has a state of circular polarization.

3.3. Determination of Angle of Incidence for 50/50 BS

Finally, we fix the gap thickness at $d_2 = 0.2\lambda_0$ ($\lambda_0 = 500\,\text{nm}$) and wavelength of the incident wave at 500 nm. The calculated R and T

Table 2. The calculated critical wavelength at some selected angles of incidence for both the TE and TM waves.

		43°	45°	50°	55°	60°	65°	70°	75°	80°	85°
d_c/λ	TE	370	393	454	520	597	696	840	1080	1564	— — —
	TM	202	263	420	592	812	1085	1476	— — —	— — —	— — —

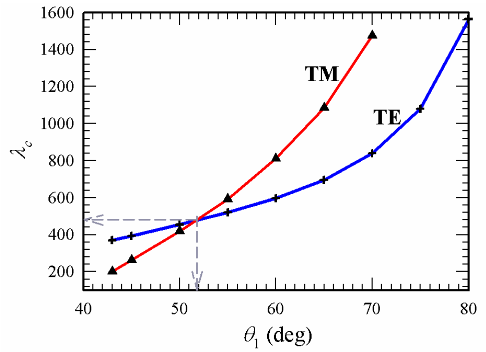

Figure 5. The calculated critical wavelength as a function of the angle of incidence for the 50/50 beam splitting. Both TE and TM curves have an crossover at $\theta_1 = 51.8°$ and $\lambda_c = 478\,\text{nm}$.

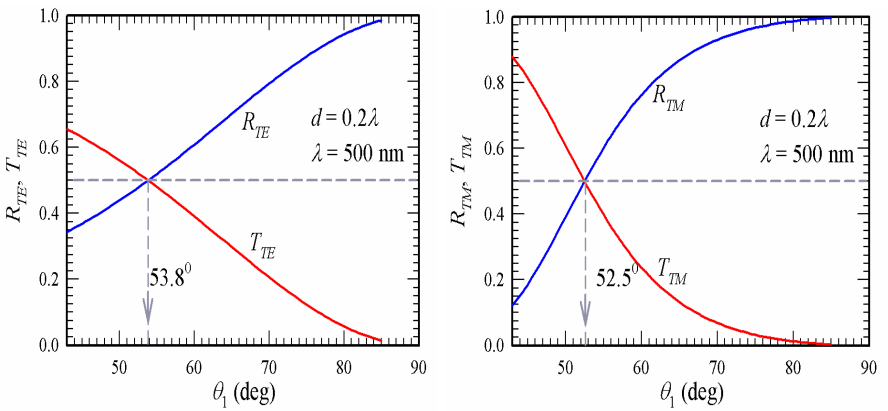

Figure 6. The calculated angle-dependent reflectance and transmittance for the TE wave and TM waves. The TE-wave critical angle is $\theta_c = 53.8°$ and TM-wave critical angle is $\theta_c = 52.5°$.

as a function of the angle of incidence are shown in Figure 6. It is seen that a 50/50 BS can be obtained at a critical angle θ_c. In TE wave, $\theta_c = 53.8°$, and it is 52.5° for TM wave, i.e., at the same gap thickness and wavelength, the critical angle for TE wave is slightly larger than that of TM wave.

4. CONCLUSION

Based on the use of the frustrated total internal reflection, a theoretical analysis on the design of a 50/50 beam splitter has been made. According to the above analyses, some conclusions can be drawn. First, at a fixed wavelength of incident wave, the gap thickness in the lower-index layer decreases with the increase in the angle of incidence. Second, at a fixed gap thickness, there exists a critical wavelength for beam splitting. This critical wavelength increases with increasing angle of incidence. Finally, at a fixed wavelength and a fixed gap thickness, the angle of obtaining 50/50 beam splitter in TE wave is slightly larger than that in TM wave.

ACKNOWLEDGMENT

C.-J. Wu acknowledges the financial support from the National Science Council (NSC) of the Republic of China (R.O.C., Taiwan) under Contract No. NSC-100-2112-M-003-005-MY3 and from the National Taiwan Normal University under NTNU100-D-01.

REFERENCES

1. Orfanidis, S. J., *Electromagnetic Waves and Antennas*, Rutger University, 2008, www.ece.rutgers.edu/_orfanidi/ewa.
2. Yeh, P., *Optical Waves in Layered Media*, John Wiley & Sons, Singapore, 1991.
3. Zhu, Y., C. Yao, J. Chen, and R. Zhu, "Frustrated total internal reflection evanescent switching," *Optics Laser Technol.*, Vol. 31, 539–542, 1999.
4. Mossman, M. A, V. H. Kwong, and L. A. Whitehead, "A novel reflective image display using total internal reflection," *Displays*, Vol. 25, 215–221, 2004.
5. Li, L. and J. A. Dobrowolski, "High-performance thin-film polarizing beam splitter operating at angles greater than the critical angle," *Appl. Opt.*, Vol. 39, 2754, 2000.

6. McCormick, F. B., F. A. P. Tooley, T. J. Cloonan, J. L. Brubaker, A. L. Lentine, R. L. Morrison, S. J. Hinterlong, M. J. Herron, S. L. Walker, and J. M. Sasian, "Experimental investigation of a free-space optical switching network by using symmetric self-electro-opticeffect devices," *Appl. Opt.*, Vol. 31, 5431–5446, 1992.
7. Ojima, M., A. Saito, T. Kaku, M. Ito, Y. Tsunoda, S. Takayama, and Y. Sugita, "Compact magnetooptical disk for coded data storage," *Appl. Opt.*, Vol. 25, 483–489, 1986.
8. Kunstmann, P. and H.-J. Spitschan, "General complex amplitude addition in a polarization interferometer in the detection of pattern differences," *Opt. Commun.*, Vol. 4, 166–168, 1971.
9. Azzam, R. M. A. and N. M. Bashara, *Ellipsometry and Polarized Light*, North-Holland, Amsterdam, 1987.
10. Wu, C.-J., T.-J. Yang, and S.-J. Chang, "Analysis of tunable multiple-filtering property in a photonic crystal containing strongly extrinsic semiconductor," *Journal of Electromagnetic Waves and Applications*, Vol. 25, Nos. 14–15, 2089–2099, 2011.
11. Wu, C.-J., M.-H. Lee, W.-H. Chen, and T.-J. Yang, "A mid-infrared multichanneled filter in a photonic crystal heterostructure containing negative-permittivity materials," *Journal of Electromagnetic Waves and Applications*, Vol. 25, No. 10, 1360–1371, 2011.
12. Hsu, H.-T., T.-W. Chang, T.-J. Yang, B.-H. Chu, and C.-J. Wu, "Analysis of wave properties in photonic crystal narrowband filters with left-handed defect," *Journal of Electromagnetic Waves and Applications*, Vol. 24, No. 16, 2285–2298, 2010.
13. Dai, X., Y. Xiang, and S. Wen, "Broad omnidirectional reflector in the one-dimensional ternary photonic crystals containing superconductor," *Progress In Electromagnetics Research*, Vol. 120, 17–34, 2011.
14. Wu, C.-J. and Z.-H. Wang, "Properties of defect modes in one-dimensional photonic crystals," *Progress In Electromagnetics Research*, Vol. 103, 169–184, 2010.
15. Wu, C.-J., Y.-H. Chung, B.-J. Syu, and T.-J. Yang, "Band gap extension in a one-dimensional ternary metal-dielectric photonic crystal," *Progress In Electromagnetics Research*, Vol. 102, 81–93, 2010.
16. Rahimi, H., A. Namdar, S. Roshan Entezar, and H. Tajalli, "Photonic transmission spectra in one-dimensional fibonacci multilayer structures containing single-negative metamaterials," *Progress In Electromagnetics Research*, Vol. 102, 15–30, 2010.

17. Kinto-Ramírez, H., M. A. Palomino-Ovando, and F. Ramos-Mendieta, "Photonic modes in dispersive and lossy superlattices containing negative-index materials," *Progress In Electromagnetics Research B*, Vol. 35, 133–149, 2011.
18. Suthar, B. and A. Bhargava, "Tunable multi-channel filtering using 1-D photonic quantum well structures," *Progress In Electromagnetics Research Letters*, Vol. 27, 43–51, 2011.
19. Rahimi, H., "Backward tamm states in 1D single-negative metamaterial photonic crystals," *Progress In Electromagnetics Research Letters*, Vol. 13, 149–159, 2010.
20. Drevko, D. R. and Y. A. Zyuryukin, "Specifics of electromagnetic TE waves splitting and combining under the conditions of frustrated total internal reflection in a thin dielectric layer," *Optics and Spectroscopy*, Vol. 108, 996–998, 2010.